AMMONIA-FREE NOx CONTROL SYSTEM

QUARTERLY TECHNICAL PROGRESS REPORT NO. 41865R6

JANUARY 1 THROUGH MARCH 31, 2005

Prepared by

Song Wu, Zhen Fan, Andrew H. Seltzer
Foster Wheeler North America Corp.,

and

Richard G. Herman
Energy Research Center, Lehigh University

Issued: April 30, 2005

Work Performed Under Contract: DE-FC26-03NT41865

For

U.S. Department of Energy
National Energy Technology Laboratory
Morgantown, West Virginia

By

Foster Wheeler North America Corp.
12 Peach Tree Hill Road
Livingston, New Jersey 07039

Disclaimers

"This report was prepared as an account of work sponsored by an agency of the United States Government. Neither the United States Government nor any agency thereof, nor any of their employees, makes any warranty, express or implied, or assumes any legal liability or responsibility for the accuracy, completeness, or usefulness of any information, apparatus, product, or process disclosed, or represents that its use would not infringe upon privately owned rights. Reference herein to any specific commercial product, process, or service by trade name, trademark, manufacturer, or otherwise does not necessarily constitute or imply its endorsement by the United States Government or any agency thereof. The views and opinions of authors expressed herein do not necessarily state or reflect those of the United States Government or any agency thereof."

Neither the author, nor any affiliate, nor any of their employees, makes any warranty, express or implied, or assumes any legal liability or responsibility including, but not limited to, in regard to the accuracy, completeness, or usefulness of any information, apparatus, product, or process disclosed, or represents that its use would not infringe upon privately owned rights whether such liability or responsibility is of a direct, indirect, special, punitive, incidental, consequential, or other nature and whether arising in contract, warranty, tort including negligence, strict liability, or other legal theory. Utilization of this information is with the above understanding.

AMMONIA-FREE NOx CONTROL SYSTEM

TECHNICAL PROGRESS REPORT NUMBER 41865R6
FOR JANUARY THROUGH MARCH 2005

Abstract

Research is being conducted under United States Department of Energy (DOE) Contract DE-FC26-03NT41865 to develop a new technology to achieve very low levels of NOx emissions from pulverized coal fired boiler systems by employing a novel system level integration between the PC combustion process and the catalytic NOx reduction with CO present in the combustion flue gas. The combustor design and operating conditions will be optimized to achieve atypical flue gas conditions. This approach will not only suppress NOx generation during combustion but also further reduce NOx over a downstream catalytic reactor that does not require addition of an external reductant, such as ammonia.

This report describes the work performed during the January 1 to March 31, 2005 time period.

Table of Contents

1.0 EXECUTIVE SUMMARY 1
1.1 Project Overview 1
1.2 Progress During the Quarter 1

2.0 EXPERIMENTAL 3
2.1 Test Rig 3
2.2 Catalyst Preparation 4
2.3 Catalyst Test Procedure 5

3.0 RESULTS AND DISCUSSIONS 8
3.1 Honeycomb Reactor versus Packed Bed of Granular Catalysts 8
3.2 Transport Phenomena and Limiting Factors of Catalyst Performance 8
3.3 External Mass Transfer 8
3.4 Distribution of Active Species in Granular Catalysts 9
3.5 Catalysts Reaction and Scale-Up Model 10
3.6 Reaction Order and Activation Energy 12
3.7 Catalyst Effectiveness Factor 13

4.0 CONCLUSION 16

5.0 REFERENCES 17

List of Figures

Figure 1 Bench Scale NOx Testing System 3
Figure 2 Cross Section of a Fresh Catalyst Particle 10
Figure 3 SEM EDX Image of Fresh Catalyst Cross Section 10
Figure 4 Effectiveness Factor as a Function of Thiele Modulus 11
Figure 5 Test Data and Model Prediction with First Order Assumption 12
Figure 6 Observed Activation Energy of Test Data 13
Figure 7 Reactant Distribution Profile for Lab and Honeycomb Catalysts 15

List of Tables

Table 1 Catalyst Samples Tested 7
Table 2 External Mass Transfer Data 12
Table 3 Pore Diffusion and Effectiveness Factor Calculation 14

1.0 EXECUTIVE SUMMARY

1.1 Project Overview

State-of-the-art NOx control technology for pulverized coal (PC) steam plants involves a combination of low NOx combustion and selective catalytic reduction (SCR) technologies. Development of these systems has approached a plateau and further improvements will likely be incremental. To advance NOx control technology to the next level, new concepts must be considered.

The objective of this project is to evaluate the viability of a novel integration between the PC combustion process and flue gas NOx reduction. The concept exploits the relationship between CO and NOx both in the combustion and flue gas NOx destruction processes to achieve very low levels of NOx from the boiler system without adding any external reductant, such as ammonia, typically used for SCR processes.

The project starts with a review and evaluation of commercial and developmental catalysts for NOx reduction and CO oxidation, including those catalysts formulations successfully used in the automotive applications, for their use in PC power plants. This knowledge, combined with prior catalyst research experience for power plant applications allows the project team to identify and test catalyst formulations robust enough for the oxidizing flue gas environment in power plants, and capable of achieving competitive NOx reduction performance and economic targets.

A detailed PC combustion study, applying computational fluid dynamics simulation program to perform boiler and burner design modeling, complements the catalyst development effort by investigating ways to optimize the combustion process for the lowest NOx formation while generating sufficient levels of CO needed by the downstream catalytic NOx reduction process. Furnace configuration, air staging, and burner design are evaluated in this process.

The study will then focus on the comparative evaluation of a conceptual, 400 MWe, coal-fired PC boiler system, utilizing this novel NOx control concept. For this evaluation, the concept plant will be compared to a traditional PC boiler configured with current low NOx combustion technology and an ammonia-based SCR system. The comparison will involve conceptual level design of the furnace and catalyst reduction system to obtain equipment pricing, operational costs, performance data as well as qualitative reliability information.

1.2 Progress During the Quarter

The project work during this quarter was primarily on Task 4 – System Conceptual Design. The work of Task 4 provides the basis for Task 5 Comparative Evaluation of performance and costs.

As the previously reported work on Task 3 - Furnace Optimization indicates, adequate CO/NOx ratios, as required by the downstream catalytic reactor, can be obtained by modifying furnace operating conditions, without significant physical changes to the burner and boiler equipment. Therefore, the design and cost impact on the furnace / boiler proper due to the new NOx control system will be minimal, and the system design effort is mainly devoted to the conceptual design of the catalytic reactor.

The basic configuration of the catalytic reactor will be an activated alumina based, honeycomb type fixed bed reactor. This configuration is selected because of its good structural strength and thermal stability. In addition, it can utilize most of the manufacturing and construction methods currently employed for conventional SCR applications, and will likely be readily accepted by the utility industry. Other configurations, such as injection – capture, fluidized bed or moving bed reactors, may be developed to deliver adequate performance and cost-effectiveness, particularly when utilizing the low cost, activated carbon based catalysts. However, these alternative configurations represent a total departure from the current SCR process and therefore may have additional hurdles to gain commercial acceptance.

The key to realistic design of a 400MWe size catalytic reactor is reliable scale-up from the small test rig in laboratory. Successful scale-up requires careful characterization and modeling of transport phenomena such as bulk mass transfer; pore diffusion and distribution of active ingredients in the substrate. These topics are the focus of the project work in the past quarter and will be described in the following sections.

2.0 EXPERIMENTAL

2.1 Test Rig

A fixed bed reactor at Lehigh University was the main experimental tool employed in this study. The catalyst testing system featured a vertical down flow quartz tube reactor (10.5 mm ID x 13 mm OD). Temperature in the reactor was monitored by an axial thermocouple located in the catalyst bed. The tip of the thermocouple is usually positioned 2.5 to 5.5 cm below the top of the catalyst bed. Heating was accomplished with a vertical split-tube furnace surrounding the reactor. The gas stream inlet and outlet 316 stainless steel sections were wrapped with heating tapes and insulation and heating was controlled by two Variacs. Temperatures of the inlet and outlet lines were monitored by six thermocouples and maintained above 100°C.

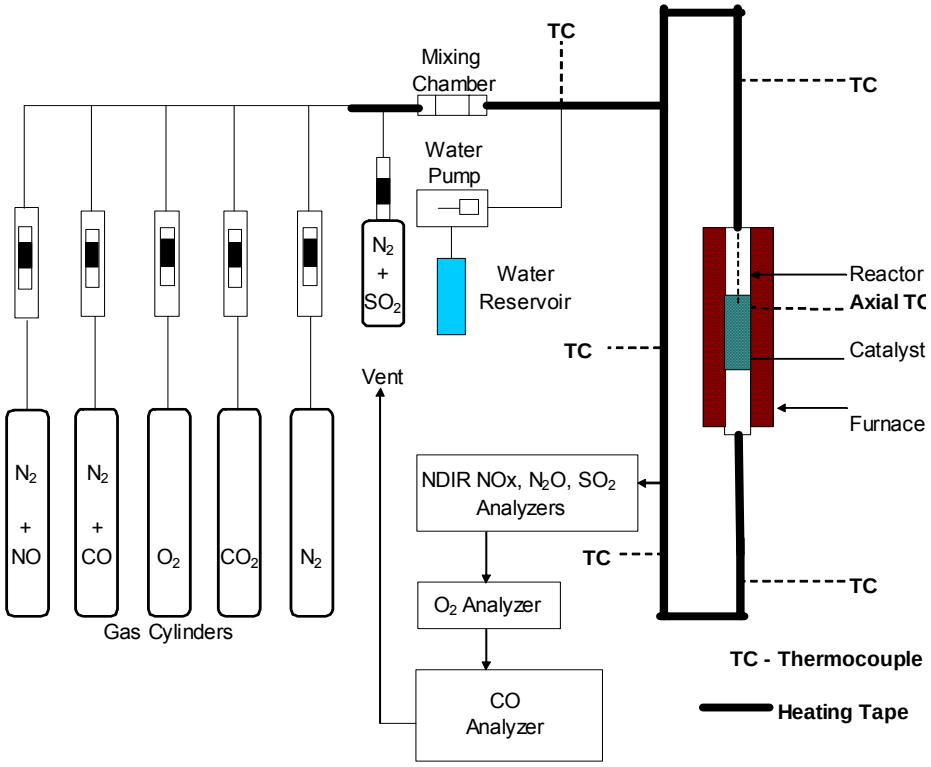

Figure 1 Bench Scale NOx Testing System

A process flow diagram of the NO reduction test rig is shown in Figure 1. Approximately 20 ml of weighed catalyst sample was placed in the reactor and supported by a quartz wool plug. Based on literature survey, the CO-NO reaction under study is not catalyzed by the quartz reactor tube at temperatures below 1000°C. Individual gas flow meters were used to regulate flow rates from gas cylinders containing NO/N_2, CO/N_2, O_2, CO_2, N_2, and SO_2/N_2 to simulate flue gas from coal-fired power plants. A cylinder pump was used to inject desired amount of distilled water through

a vaporizing pipe section into the heated inlet gas line to the reactor. The outlet test gas goes through a chiller before entering the gas analyzers. A bypass valve can be used to connect the inlet gas stream directly to the analyzers to check and confirm the inlet concentrations of NO and other gases. A bubble flow meter was used to calibrate the rotameters for individual gas streams.

Analysis of the NO, N_2O, and SO_2 concentrations in the gas stream were achieved with a Siemens Ultramat 6 non-dispersive infrared (NDIR) analyzer, while O_2 was analyzed by a Siemens Oxymat 6 Paramagnetic analyzer. CO was determined by a Testo 325-3 digital CO analyzer. Monitoring of these gases in the reactor inlet and outlet streams was carried out to determine if these components of the gas mixture were being generated or consumed. Moisture CO_2, and N_2 concentrations were calculated based on their flow rates into the reactor.

2.2 Catalyst Preparation

The activated carbon (AC) used in this study was a 12-20 mesh size product purchased from Aldrich. It was lignite-derived, designated as Darco Activated Carbon and manufactured by American Norit Co. Due to its relatively low cost, lignite-based activated carbon has been widely used in the waste to energy industry for trace pollutant removal, and is currently being demonstrated to capture mercury for coal fired utility plants. The BET surface area of an "as received" AC sample was determined (6-point analysis) by nitrogen adsorption at -196^{o}C using a Micromeritics Gemini 2360 V1.03 instrument. Before analysis, the sample was purged with flowing N_2 while heating from 60^{o}C to 200^{o}C over a period of 55 min. The sample was then maintained at 200^{o}C for 2 hr and cooled to ambient temperature. During this thermal treatment, the sample exhibited a 1.5 wt% loss of weight. The determined surface area of the activated carbon was 525 m^2/g. After loading of the catalytic components the surface area for catalyst Type B became 468 m^2/g, which is very close to that of the as received AC.

Another catalyst substrate used was activated alumina (AA). An 8-14 mesh size activated alumina (AA) product was obtained from Fisher Scientific. It was designated as A-505 adsorption grade alumina. The alumina was utilized either *as received*, or *after calcining.* The as received sample was simply purged with N_2 and stored in a N_2-filled glove bag containing a beaker of Drierite to maintain a dry atmosphere before catalyst preparation. To obtain a calcined sample, a portion of the alumina was placed in a porcelain evaporation dish and placed in a furnace at 180^{o}C. The temperature was increased to 500^{o}C, and the sample was held at this temperature overnight. It was then removed from the furnace, cooled, and placed in a N_2-filled glove bag containing a beaker of Drierite to maintain a dry atmosphere. A small portion of the activated alumina in a separate dish with the same calcination treatment exhibited a 14.4 % wt loss. The BET surface areas of the alumina samples used as substrate are given in Table 2.

The preparation procedure of the AA catalyst followed that utilized previously for the Fe/Cu/AC catalysts, by an impregnation method. Reagent grade chemicals of metal nitrates from Fisher Scientific (ACS Certified) or Strem Chemcials were dissolved in distilled water and heated to 60^{o}C. To the solution was added AL while maintaining constant stirring. The solution was then evaporated over a period of a few hours, and when the solid was dry to the touch, it was placed in a plastic bottle. The open plastic bottle was placed in an N_2-filled glove bag containing a beaker of Drierite desiccant for further drying.

Activation of catalysts was carried out by decomposition of metal salts. The impregnated multi-metal nitrate salts were decomposed by heating under established flow rates of the simulated gas mixture containing approximately 3.0% O_2, 14% CO_2, 520 ppm CO, and balance N_2. The gas hourly space velocity (GHSV) used for the decomposition treatment was about 930 hr^{-1}. The inlet and exit lines as well as the furnace were then heated. Usually, the catalyst was slowly heated to about 270^oC over a period of 3-6 hr and maintained at this temperature for 0.5-3 hr until the emitted NO achieved low levels.

During this treatment, a large amount of NO was released from the catalyst, as a result of nitrate salt decomposition, which peaked in the temperature range of 100-200^oC and then decreased with further increase of temperature and time of equilibration. CO, O_2, and N_2O were also measured during decomposition/activation at increased temperatures. After the decomposition treatment, the furnace controller was turned off and only the flow of N_2 was maintained overnight as the furnace cooled to ambient temperature.

2.3 Catalyst Test Procedure

For NO reduction activity determination, the flow rates of the gas mixture components were reestablished and the flow rates were measured/confirmed by means of a bubble meter. The reactor was then heated and the NO/N_2 flow was turned on. The temperature of the catalyst bed was then sequentially changed to obtain a conversion-temperature profile both in steady state and in transient conditions. To screen the performance of different catalysts, a constant GHSV of 1050 hr^{-1} at ambient temperature and pressure and the inlet gas composition was used. The established dry reactant gas mixture consisted of the following for most of the tests:

NO	CO	O_2	CO_2	N_2
260 ppm	520 ppm	3.0 %	14.0%	83%.

This gas mixture gives a CO/NO molar ratio of 2.0, with enough excess reductant for the NO reduction reaction. To study the catalyst reactivity for NO reduction without the interference of poisoning or inhibition, the initial catalyst evaluation tests were carried in the absence of SO_2 and moisture. After the initial tests, selected catalysts were exposed to the reactant gas stream containing moisture and SO_2 to determine inhibition and poisoning effects.

For experiments with moisture added to the gas stream, water was injected and vaporized to give the following reactant gas mixture with an overall GHSV of 1140 hr^{-1}:

NO	CO	O_2	H_2O	CO_2	N_2
240 ppm	480 ppm	2.8 %	8.0%	12.9%	76.3%.

When the reactant stream contained SO_2, a 5727 ppm SO_2/N_2 mixture was utilized and its flow rate was compensated by decreasing the N_2 flow rate accordingly to maintain the overall GHSV at 1140 hr^{-1}. The resultant reactant gas mixture consisted of:

NO	CO	SO_2	O_2	H_2O	CO_2	N_2
240 ppm	480 ppm	200 ppm	2.8 %	8.0%	12.9%	76.3%.

Catalytic reactivity is expressed by conversions, where the calculated conversions are multiplied by 100 to obtain % Conversion, i.e.

NO	Conversion = $1 - (NO)_{out} / (NO)_{in}$
N_2O	Conversion = $2(N_2O)_{out} / (NO)_{in}$
CO	Conversion = $1 - (CO)_{out} / (CO)_{in}$
O_2	Conversion = $1 - (O_2)_{out} / (O_2)_{in}$
SO_2	Conversion = $1 - (SO_2)_{out} / (SO_2)_{in}$

It was assumed that there was no significant difference between gas inlet and outlet in its molar flow rates, considering that about 97% of the dry feed gas is N_2 or CO_2, neither of which are expected to participate in any of the reactions under study here. The NO reduction levels were determined following attainment of steady state. As a post-combustion NO control process, a low NO level of 260 ppm was used in this test, assuming some form of low NOx combustion technology is already being used.

The temperature of the catalyst bed was changed and the NO conversion was determined as it approached to a steady state at each set point. The set point temperatures were selected to achieve the maximum NO reduction for each catalyst. The NOx conversion as a function of temperature and time were recorded. The other gases, such as O_2, CO, SO_2, and N_2O, were also recorded. They are used to analyze catalytic selectivity, NOx reduction pathways, and possible side reactions, especially the relations among NOx reduction, CO depletion, and O_2 consumption. The reactivity profile of NOx reduction *vs*. temperature can then be plotted to compare the performance from different catalysts.

After a test, the test sample was cooled down and preserved in an N_2 environment for subsequent characterization. Most of the tested catalysts were subjected to repeat test(s) under identical conditions as used for the first day test. The multi-day tests ensure data/procedure repeatability and provide clues to any deactivation over time on stream.

Tests on various combinations of Fe, Cu, Ce, and K on the AC and AL supports have been conducted. To date, 13 catalysts have been prepared and evaluated.

Table 1 describes the various catalyst samples tested. The amount of each metal impregnated on the AC or AA support is expressed as the percentage of a reference total metal loading. The test runs in this report are reported as a combination of letters and numbers, such as A-1, B-2, where the letter indicates the catalyst type tested and the number indicates the order of the test run, for example, 1 for first run (e.g. Day 1). Duplicate samples of some of the catalysts were tested under different conditions and designated with different names for convenience of reference. P is a sample of the remaining O catalysts after eight tests at a GHSV of 1050 1/hr. It is used for high GHSV testing at 5250 1/hr.

Table 1. Catalyst Samples Tested*

Catalyst Name	First Test Date	Catalyst Formula	GHSV, l/hr	Substrate
A	4/07	As-received AC	1050	AC
B	4/09	10% Fe/10% Cu	1050	AC
C	4/21	40% Fe/10% Cu	1050	AC
D	4/30	10% Fe/30% Cu	1050	AC
E	5/21	40% Fe/0% Cu	1050	AC
F	5/26	7% Fe/7% Cu	840	AC
G	5/29	40% Fe/10% Cu	1050	AC
H	6/09	40% Fe/30% Cu	1050	AC
I	6/22	Aqueous-treated AC	1050	AC
J	6/29	40%Fe/30%Cu/20% Ce	1050	AC
K	7/22	40% Fe/30% Cu/20% K	1050	AC
L (duplicate of E)	8/13	40% Fe/0% Cu	1050	AC
M (duplicate of H)	9/02	40% Fe/30% Cu	1050	AC
N	10/04	40% Fe/30% Cu	1050	AA
O	11/05	40% Fe/30% Cu	1050	AA (calcined)
P (previously tested O)	12/09	40% Fe/30% Cu	5250	AA (calcined)
Q (duplicate of O)	12/16	40% Fe/30% Cu	5250	AA (calcined)
R (duplicate of H)	01/07	40% Fe/30% Cu	5250	AC (calcined)

* Percentage in catalyst formula refers to a reference total loading.

3.0 RESULTS AND DISCUSSIONS

3.1 Honeycomb Reactor versus Packed Bed of Granular Catalysts

Alumina-based honeycomb monolith reactor is selected as the base case for reactor design. The honeycomb configuration is one that is typical for SCR catalysts, with 7.1 mm pitch, 0.7 mm wall thickness, and 1 m monolith length. The honeycomb is prepared by mixing powders of substrate material, active species and binder material into a homogeneous paste and extruding the paste into monolith form.

As described in the previous section, the catalysts tested in the packed bed rig are activated alumina granules impregnated with active species. The granular material has irregular shape and a median particle size of 1.88 mm. Since the active species are loaded with aqueous impregnation method, a non-uniform distribution of the impregnated species can be expected.

3.2 Transport Phenomena and Limiting Factors of Catalyst Performance

The following transport steps help to determine the catalytic reactor system performance:

- Mass transfer from bulk flow to the outer surface of catalyst.
- Distribution / penetration of active components into the substrate structure. This is particularly important in the case of granular catalysts where active species (e.g. CuO and Fe_2O_3) are impregnated into the substrate.
- Diffusion of reactants (NO and CO) through the catalyst structure to reach inner active sites. The prepared catalysts must have not only sufficient pore volume, but also pores with adequate diameter and free path length to facilitate this diffusion.
- Adsorption of reactants on active sites on the pore surface.
- After reaction, diffusion of the products back to the bulk flow.
- For bi-function, redox catalysts, such as those studied here, the transfer of oxygen between the reducing sites and the oxidizing sites can be an additional limiting factor. The effectiveness of this transfer step is affected by the distance between the two types of sites, which is in turn determined by the relative distribution and density of active species in the substrate structure.

The external mass transfer can be calculated using empirical correlations for various catalyst configurations. The other transport steps described above can be considered using an effectiveness factor, which is defined as (Dogu 1986),

η = (observed reaction rate / reaction rate if all sites were at external surface conditions)

3.3 External Mass Transfer

To determine the relative importance of external mass transfer, calculations were made for both the packed bed test of granular catalysts and honeycomb reactor. Mass transfer in the fixed bed reactor was calculated from the following equation (Kunii and Levenspiel 1991),

$$Sh = 2 + 1.8\, Re^{1/2}\, Sc^{1/3} \quad (1)$$

Intra-channel mass transfer of honeycomb monolith was estimated by Equation 2 (Gilliland 1934), and Equation 3 (Holmgren and Andersson, 1998), separately,

$$Sh = 0.023\, Re^{0.83}\, Sc^{0.44} \quad (2)$$

$$Sh = 3.53 \exp[0.0298 Re(d_h/L) Sc] \quad (3)$$

where, d_h and L are hydraulic diameter and length of the monolith channels respectively.

Assuming an inlet concentration of 250 ppm and 80% catalytic reduction of NO, the mass transfer data is summarized in Table 2, for both the test rig and a 400 MWe size honeycomb reactor.

Table 2 External Mass Transfer Data

	Packed Bed Test Rig	Honeycomb by Eq. 2	Honeycomb by Eq. 3
Sherwood Number, -	6.5	8.3	4.5
Mass Transfer Co., m/s	1.3E-01	4.9E-02	2.6E-02
Mass Transfer Limit, L_m, kg/s	8.0E-07	1.59	0.86
Total NO Reduced, F_{no}, kg/s	1.6E-09	0.10	0.10
L_m / F_{no}, -	515.7	15.3	8.3

Clearly, the external mass transfer resistance for the packed bed case is negligible. Even for the honeycomb reactor the external mass transfer limit is an order of magnitude larger than the NO reduction rate. Therefore external mass transfer is not a significant rate-limiting factor for the overall reaction.

3.4 Distribution of Active Species in Granular Catalysts

When the catalyst is prepared by the impregnation method, dissolved salts in the solution diffuse through the outer surface into inner pores, and in the mean time they are adsorbed or deposit on the pore walls physically and/or chemically. This diffusion-adsorption process generates a density distribution for active components, which is high near the particle surface and reduces with depth into the particle. Figure 2 is a photo of the cross section of a fresh catalyst particle taken with an optical microscope. Figure 3 is a SEM EDX image of the cross section of a similar particle. Both figures clearly show that only a thin outer layer of the substrate is fully penetrated by active components. SEM EDX spectrum analysis of various spots on the cross section also revealed different penetration patterns for CuO and Fe_2O_3 into the alumina substrate: Fe_2O_3 tends to concentrate in a thin shell while CuO tends to diffuse deeper into the particle.

These image analyses also indicate that the granular catalysts used for our laboratory testing can be greatly improved by homogeneously distributing both metal oxides, so that the optimum ratio of the active species can be achieved for the entire volume of the substrate material, thus maximizing the catalyst utilization, reducing required catalyst volume and reactor pressure drop.

Using the aqueous impregnation method, deeper and more uniform distribution can be obtained by using a longer impregnation time, and by using vacuum to withdraw air from the bare support material before impregnation. Since honeycomb elements are made from uniformly blended fine powders of support material, binder and active components, they have inherently homogeneous distribution. Therefore the commercial scale reactor with honeycomb catalysts will have higher activity on volume basis than the granular catalysts tested in laboratory.

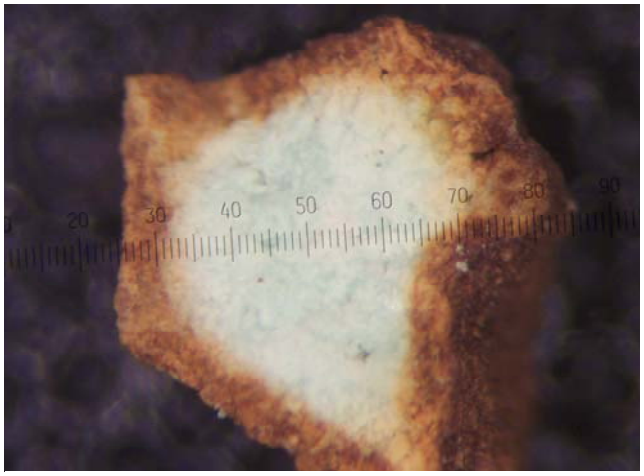

Figure 2 Cross Section of a Fresh Catalyst Particle

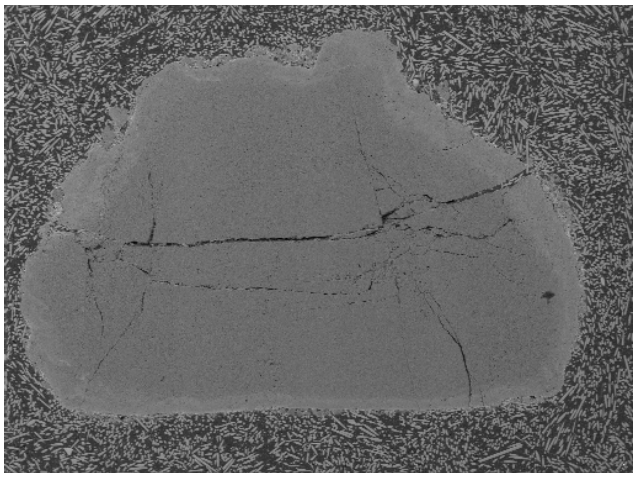

Figure 3 SEM EDX Image of Fresh Catalyst Cross Section

3.5 Catalysts Reaction and Scale-Up Model

By introducing the effectiveness factor η, a general differential catalytic reaction model can be written as,

$$-F\cdot dC_A = \eta\cdot r_w\cdot dw = \eta\cdot k_w\cdot f(C_A)\cdot dw = \eta\cdot k_w\cdot f(C_A)\cdot\rho\cdot dV \qquad (4)$$

Here F represents the gas volume flow; C_A is the reactant concentration; $r_w = k_w\cdot f(C_A)$ is the reaction rate per unit mass loading of active component; $f(C_A)$ is a function of C_A depending on reaction order and stoichiometry; η is catalytic effectiveness factor defined in section 3.2; $dw = \rho\cdot dV$ is the total mass loading of active components; and ρ is the loading density of active component(s). Solving this differential equation, one will get,

$$-g(x) = -\int (dC_A)/f(C_A) = \int \eta\cdot k_w/F\cdot\rho\cdot dV = \eta\cdot k_w\cdot\rho\cdot V/F \qquad (5)$$

where x is the fractional conversion of the reactant; g(x) is a function of x, which becomes ln(1-x) for first order reactions.

To get the same g(x), the value of the right hand side of equation (5) has to be kept the same. This means that, for a given type of catalyst, same performance (conversion) can be obtained as long as the parameter group $\eta \cdot k_w \cdot \rho \cdot V/F$ is kept constant. Therefore, this parameter group represents the scale-up rule for catalytic reactor. For homogeneous catalysts with given η, k_w, and ρ, the scale-up rule is simplified as V/F, which is catalyst volume based space time (the reciprocal of space velocity). For catalysts with a coating layer of active components, $V = S \cdot \delta$, where S is the external surface area of the coating layer and δ is the coating thickness. With given η, k_w, ρ, and δ, the scale-up rule becomes F/S, which is the catalyst external surface based area velocity U_s.

Catalyst activity is affected by active component concentrations, their ratios and distributions. The effective factor η is in fact a measure of the rate of intra-catalyst transport (represented by an effective diffusion coefficient D_{eff}) against the true reaction rate occurring at active sites (k_v), which is a function of temperature for a given catalyst. Solution of the steady state differential equation for the mass conservation of reactant diffusing through the catalyst structure leads to the expression of η as a function of φ, where φ is the Thiele modulus. For first order reactions, $\varphi = (k_v/D_{eff})^{1/2} \cdot \delta$, where δ is the equivalent penetration depth. η can be expressed as,

$$\eta = \tanh \varphi / \varphi \qquad (6)$$

As shown in Figure 4, η approaches one for very small φ values, and $1/\varphi$ for large φ values.

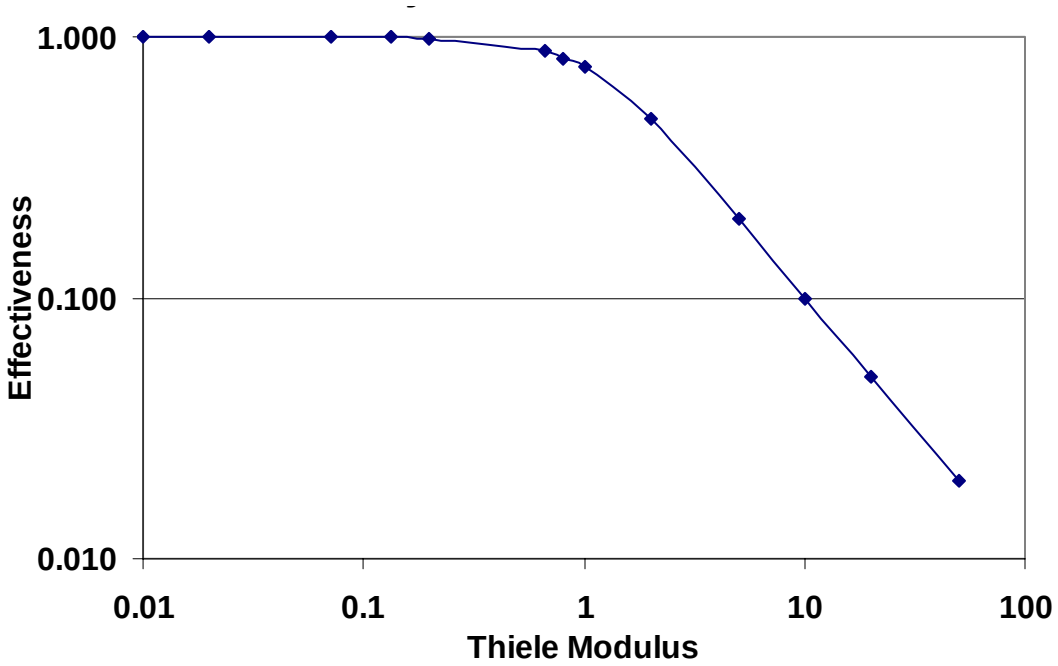

Figure 4 Effectiveness Factor as a Function of Thiele Modulus

In a complex system, such as those with redox catalysts, the density distributions of active components affect the reaction rate or activity. Let,

$$\eta \cdot k_w \approx A_\eta \cdot e^{-E/RT} \qquad (7)$$

The observed reaction activation energy from equation (7) will be a good index to study the parameter group $\eta \cdot k_w$, which can be calculated from equation (5) with given $\rho \cdot V/F$ and g(x) from test data.

If the catalytic reaction is under the pore diffusion limitation (with very large φ), the observed activation energy E will be only half of the true reaction activation energy E_t ($E = E_t/2$). Any change in φ (or η) will cause E to change between $E_t/2$ to E_t. Only when $\eta \approx 1.0$, E will remain nearly constant ($E \approx E_t$) as φ changes.

3.6 Reaction Order and Activation Energy

Different reaction orders can be applied to Equation 5. For example, for the first order chemical reaction, $f(C_A) = C_A$ and $g(x) = \ln(1-x)$. The test data have been plotted in the form of conversion versus reaction temperature, as shown in Figure 5. Included in the same chart are curves of predicted x for various test conditions by the catalyst reaction model. After trying different reaction orders, it was determined the model with first order assumption gives the best fit for the data, as shown in Figure 5.

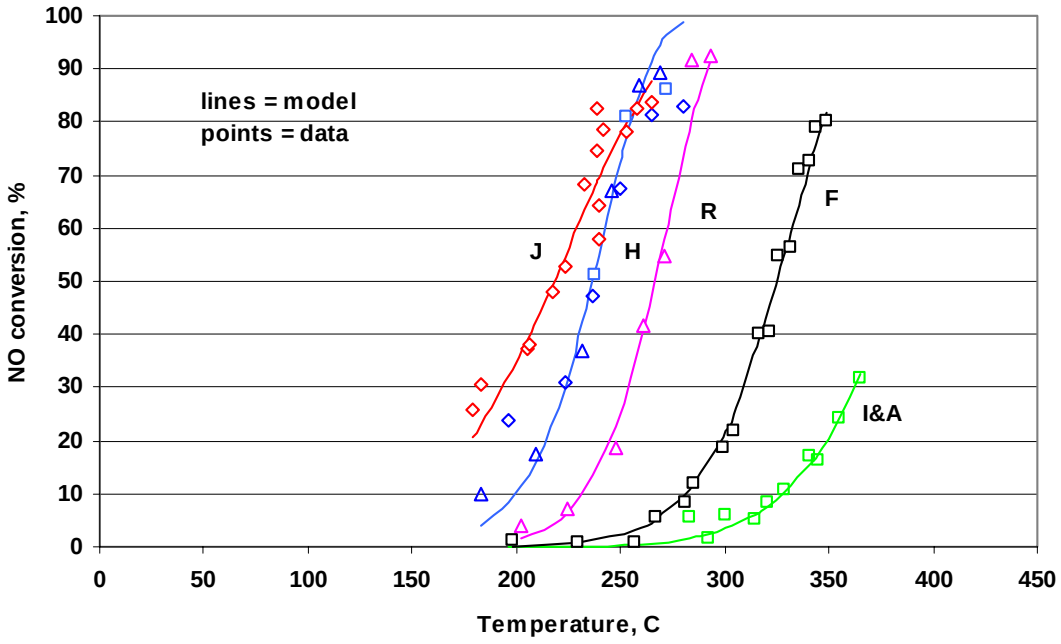

Figure 5 Test Data and Model Prediction with First Order Assumption

The observed activation energy for each test can be obtained by plotting $\eta \cdot k_w$ vs. the reciprocal of reaction temperature, as shown in Figure 6, in which the line slopes represent E/R with the unit K. All data series in Figure 6, with the exception of J and K, demonstrate an activation energy E/R of approximately $13x10^3$ K. This activation energy means that the reaction rates for these catalysts double every time the reaction temperature is increased for about 15 K, in the temperature range tested. This is comparable with the rate of the typical, kinetically controlled reactions, which as a rule of thumb doubles for every 10 K temperature rise.

Type J and Type K catalysts contains cerium and potassium respectively. As shown in Figure 6, the additional promoters Ce ad K lower the observed E/R, to about 30-40% of that of other catalysts.

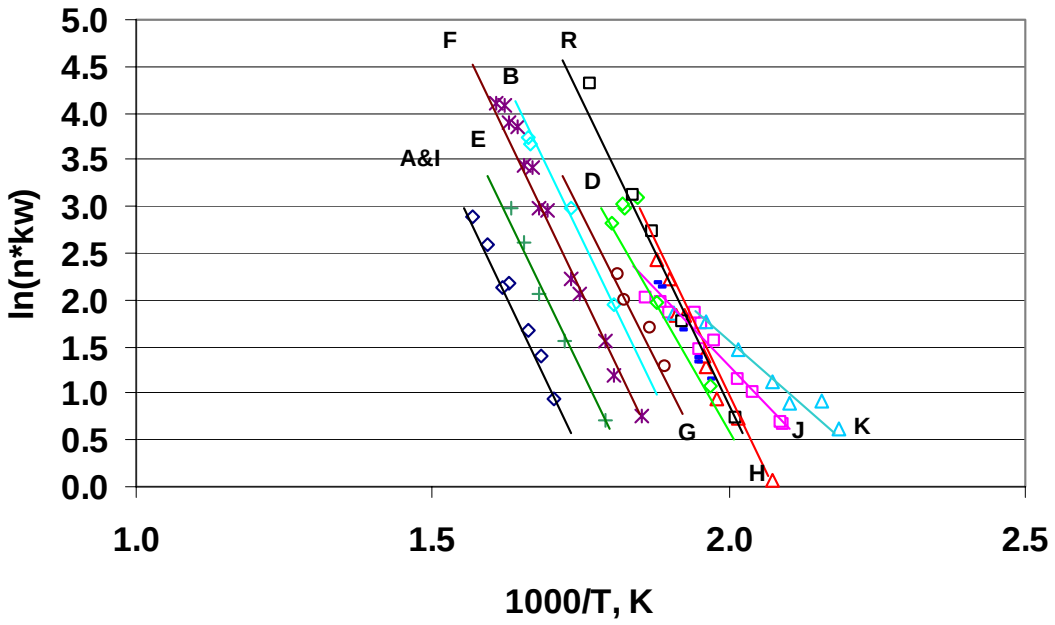

Figure 6 Observed Activation Energy of Test Data

3.7 Catalyst Effectiveness Factor

From the discussions in section 3.5, one can see that direct determination of the effectiveness factor involves iteration of Equations 5, 6 and a given effective diffusion coefficient (D_{eff}) value. Because D_{eff} is unknown for the tested catalysts, indirect methods based on in-depth test data analysis were used to infer the approximate range of the effectiveness factors.

Data series H and R were obtained under different space velocities (5250 1/hr for R and 1050 1/hr for H) with the exact same catalyst (see Table 1). Because of the 5:1 ratio in space velocity (F/V), it is expected that higher reaction temperature (and therefore higher k_w) will be needed for series R to achieve the same NO conversion than series H. Based on Equation 5, series R must have five times higher $\eta \cdot k_w$ to get the same conversion level as series H.

On the other hand, the test data show that T_{50} (reaction temperature for 50% conversion) for series R is 27 ºC higher than H. Using observed activation energy, the temperature increase is related to a 4.5 time increase in k_w, indicating η is about the same for both H and R, and in both cases very close to one.

Using $\eta \cdot k_w$ of 4.5 to 5, one can also estimate the change of φ from H to R is about 2.1 – 2.2 times, since $\varphi = (k_v/D_{eff})^{1/2} \cdot \delta$, and D_{eff} is relatively insensitive to the small temperature change. This magnitude of change in φ without causing large change in η is only possible when φ is very small (predominantly reaction rate limitation) and η is very close to 1.

Now, in order to estimate how close η is to1, one can make reasonable approximations of D_{eff}. One way is to use the Knudson diffusion coefficient, which can be calculated based on pore size and temperature (Dogu 1986). Knudson coefficient describes the diffusion through capillary (with pore-radius-to-mean-free-path-ratio typically less than 0.1), and represents the lower limit of effective diffusion coefficient, D_{eff}, which includes the effect of both Knudson diffusion and ordinary molecular diffusion.

Table 3 summarizes the calculated D_k and η_k. The pore surface area and volume data are from Perry and Chilton (1973). With the diffusion coefficient, η can be calculated from test data by iterating Equations 5 and 6. The effectiveness factors given below are for series H and O data at 50% NO conversion.

Table 3 Pore Diffusion and Effectiveness Factor Calculation

Type of Substrate	Pore Surface Area, m^2/g	Pore Volume ml/g	Pore Radius, Å	Knudson Diff. Co. D_K, cm^2/s	Effectiveness Factor η_k , -
AC	525	0.59	22	0.0093	0.96
AA	175	0.39	45	0.0185	0.98

Since D_k represents the lower limit of D_{eff}, the true effectiveness factors will be even higher than the values in Table 3. By comparative analysis of the data series for the same catalyst tested under different space velocities, for example H and R, or O and P, D_{eff} was estimated to be about 0.04 for catalysts with AC support and 0.07 for those with AA support, in the tested temperature range. With these D_{eff} values, the effectiveness factors can be determined as over 99% for all tests at low space velocity and over 96% for the tests at the high space velocity.

With the estimated diffusion coefficient, the reactant concentration distribution from the bulk flow to the center of the catalyst element can be determined. Figure 7 depicts the relative NO concentration profile for the granular AA catalyst in lab testing as well as the honeycomb configuration to be used for commercial scale design, assuming a D_{eff} of 0.07 cm^2/s.

It is clear that both external mass transfer and pore diffusion are not significant limiting factors for the reaction in both laboratory and honeycomb reactor cases. The above analysis indicates very high catalyst effectiveness was achieved during laboratory tests and the granular catalysts displayed a volume-dependant activity behavior. Because the catalysts had only limited penetration by active components, catalytic performance can be further improved by uniformly

distributing active components in the substrate structure. Also because of the high catalyst effectiveness observed from the test data, increasing the active component loading will be an effective way to raise activity of the catalyst. The commercial application will use a honeycomb configuration with homogenous chemical composition and with the flexibility to load various levels of active components. Therefore, the commercial honeycomb catalysts can be designed with high reactivity and effectiveness.

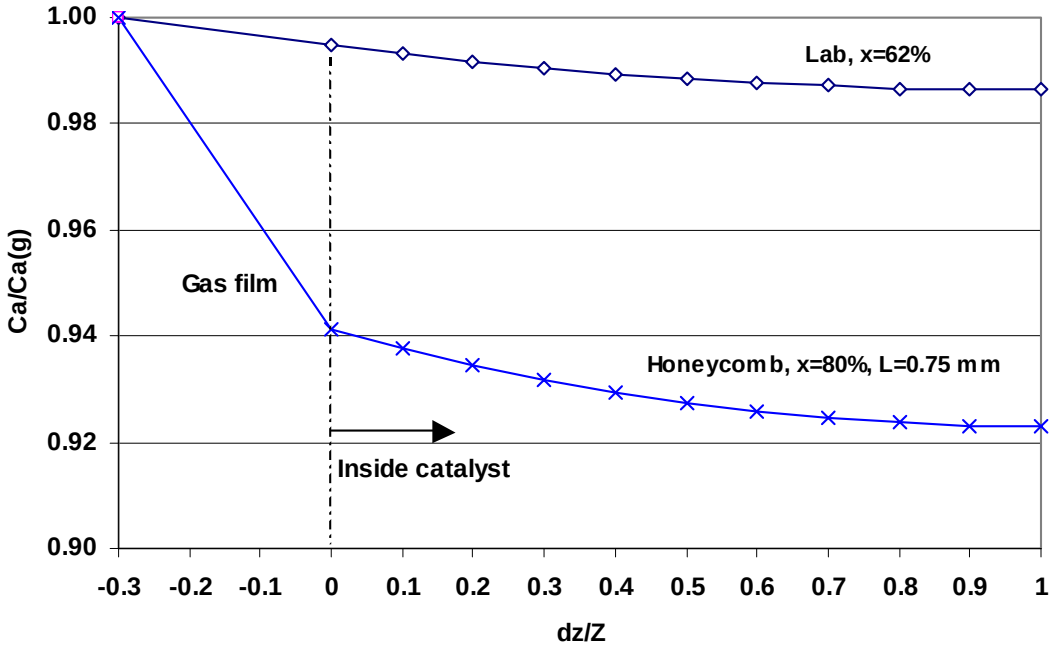

Figure 7 Reactant Distribution Profile for Lab and Honeycomb Catalysts

4.0 CONCLUSION

The previously reported laboratory test data have been further analyzed with detailed evaluation of transport and reaction steps. A catalyst reaction model was used to interpret the test data and for scaling–up to commercial size reactor with honeycomb catalysts. The following conclusions and observations can be made;

- External mass transfer resistance is negligible for laboratory packed bed tests of granular catalysts; it is also not a significant rate-limiting factor for the commercial reactor with the selected honeycomb configuration.
- Microscopic study of laboratory test samples reveals that activated components are concentrated in a thin outer shell, with limited penetration into substrate structure.
- The catalyst model with first order reaction fits well with test data. The data also demonstrated consistent observed activation energy.
- Catalyst effectiveness η is close to 1.0 for tested catalysts. The catalyst performance was not limited by pore diffusion. Honeycomb catalysts prepared based on the above findings will be able to achieve high activity and effectiveness.

The test data analysis and reaction modeling provide the foundation for further development and design of catalysts for commercial applications.

5.0 REFERENCES

Dogu, G., "Diffusion Limitations for Reactions in Porous Catalysts", in *Handbook of Heat and Mass Transfer - Volume 2: Mass Transfer and Reactor Design*, edited by Cheremisinoff, N.P., Gulf Publishing Company, 1986.

Gilliland, E.R., "Diffusion Coefficients in Gaseous Systems ", Ind. Eng. Chem., Vol.26, p.681, 1934.

Kunii, D., and Levenspiel, O., *Fluidization Engineering*, 2nd edition, Butterworth-Heinemann, 1991.

Holmgren, A., and Andersson, B., " Mass Transfer in Monolith Catalysts – CO oxidation Experiments and Simulations", Chemical Engineering Science, Vol. 53, No.13, p.2285, 1998

Perry, R. H., and Chilton, C.H., *Chemical Engineers' Handbook,* 5th edition, McGraw-Hill Book Company, 1973